Preliminary Study of a Thermal-Hydraulic Model for Helically Coiled Once-Through Steam Generator Design Analysis

Nhan Hien Hoang, Jinwook Choi, Sera Jeon, Seong-Su Jeon*
FNS Technology Co., Ltd., 13 Heungdeok 1-ro, Giheung-gu, Yongin-si, Gyeonggi-do, Repulic of Korea
E-mail: ssjeon@fnctech.com

***Keywords : Helical steam generator, HCOTSG, MRX, VISTA.**

1. Introduction

A helically coiled once-through steam generator (HCOTSG) is a compact heat exchanger in which feedwater is converted directly into superheated steam through the helically wound tubes as illustrated in Fig. 1. Owing to their compactness, high power density, and simplified system integration, HCOTSGs have been adopted for various advanced reactor systems, especially small modular reactors–SMRs (e.g., NuScale, SMART, and i-SMR) high-temperature gas-cooled reactors–HTGRs (e.g., Fort St. Vrain, HTTR, and HTR-10), and sodium-cooled fast reactors–SFRs.

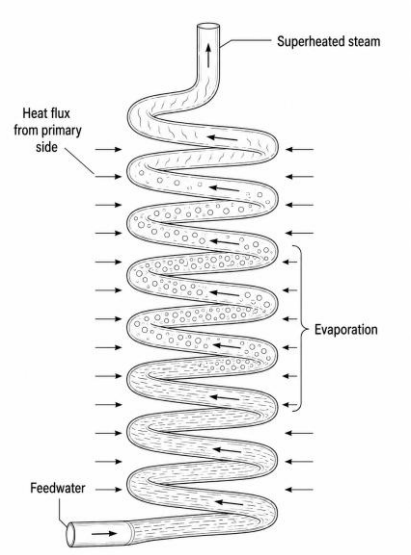


Fig. 1 Illustration of a HCOTSG

The thermal-hydraulic design of a HCOTSG involves determining the tube geometry, shell geometry, and tube arrangement required to achieve a target power over a specified range of operating pressure and temperature. Therefore, a reliable design and analysis tool is essential. Two major approaches have been used for the HCOTSG thermal-hydraulic analysis. One approach uses fixed-boundary volumes, such as the analyses using system codes (e.g., RELAP5, MARS-KS, and SPACE) [1]. The other approach uses moving-boundary volumes to overcome abrupt changes in thermal properties, flow dynamics, and heat transfer at the transition between different heat transfer regimes [2].

The moving-boundary approach generally employs the homogeneous flow model with different physical models tailored to the characteristic heat transfer regions of an HCOTSG. The primary concern of this method is the reliability of the selected physical models. Numerous physical models have been developed for tube-side (secondary) pressure drop and heat transfer, whereas relatively few models are available for the shell side (primary). Furthermore, published experimental investigations of HCOTSG thermal-hydraulic behaviors remain limited, and most experiments have been conducted using highly simplified test sections containing only a small number of tubes.

In this study, reliable physical models for HCOTSG analysis are incorporated into a thermal-hydraulic model based on the moving-boundary approach proposed by Yoon et al. [2]. Detailed verification and validation are performed to identify the most suitable combination of physical models for HCOTSG design and analysis.

2. HCOTSG Thermal-Hydraulic Model

The characteristics of a HCOTSG, as illustrated in Fig. 1, are the single-phase convective heat transfer in the primary side and the heat transfer transition along the helical tubes, from convective heat transfer to liquid in the economizer region to nucleate boiling heat transfer and mist heat transfer in the evaporation region, and to convective heat transfer to vapor in the superheated region. To simulate the HCOTSG, the following framework is established based on the homogeneous flow model [3].

Continuity:

$$W_p = const. \tag{1}$$

$$W_s = const. \tag{2}$$

Energy conservation:

$$dQ_i = W_p\left(h_{p,i} - h_{p,i+1}\right) = W_s\left(h_{s,i} - h_{s,i+1}\right) \tag{3}$$

$$T_{p,i} = ASME\left(P_{p,i}, h_{p,i}\right) \tag{4}$$

$$T_{s,i} = ASME\left(P_{s,i}, h_{s,i}\right) \tag{5}$$

Pressure drop (both sides):

$$\Delta P_i = \Delta P_{a,i} + \Delta P_{f,i} + \Delta P_{g,i} + \Delta P_{k,i} \tag{6}$$

$$\Delta P_{a,i} = \left(G^2/\rho\right)_{i+1} - \left(G^2/\rho\right)_i \tag{7}$$

$$\Delta P_{f,i} = f\left(\frac{L_i}{D_h}\right)\left(\frac{G^2}{2\rho}\right)\phi_{lo}^2 \tag{8}$$

$$\Delta P_{g,i} = \rho_i g L_i \tag{9}$$

$$\Delta P_{k,i} = K\frac{G|G|}{2\rho_f}\phi_{lo}^2 \tag{10}$$

$$\phi_{lo}^2 = \left[1 + x_e\left(\frac{\rho_f}{\rho_g} - 1\right)\right]\left[1 + x_e\left(\frac{\mu_f}{\mu_g} - 1\right)\right]^{-1/4} \quad (11)$$

$$\rho_i = \left[x_{e,i}/\rho_g + \left(1 - x_{e,i}\right)/\rho_f\right]^{-1} \quad (12)$$

$$x_{e,i} = \left(h_i - h_f\right)/h_{fg} \quad (13)$$

Thermal-sizing:

$$dQ_i = F \times U \times \Delta T_{LMTD} \times dA_{o,i} \quad (14)$$

$$\frac{1}{U} = \frac{1}{h_{i,i}}\frac{d_o}{d_i} + \frac{d_0}{2k_{w,i}}\ln\left(\frac{d_o}{d_i}\right) + \frac{1}{h_{o,i}} \quad (15)$$

In this framework, both the primary and secondary sides are discretized into cells, with each cell bounded by two nodes. The nodes are numbered sequentially from the tube inlet to the tube outlet. Pressure (P), fluid temperature (T), and mass flow rate (W) are evaluated at both the nodes and cell centers. Fluid properties, vapor quality, heat-transfer coefficients (h_i, h_o, and U), heat-transfer rate (Q), and tube-wall temperature (T_w) are evaluated at the cell centers. The calculation procedure is illustrated in Fig. 2. The starting point of the calculation for each side is determined by the specified boundary conditions.

For each cell i, the program calculates the heat-transfer rate at the outer tube surface ($Q_{o,i}$), the heat-transfer rate obtained from Eq. (14), and the heat-transfer rate at the inner tube surface ($Q_{i,i}$). The converged heat-transfer rate is determined using the value calculated from Eq. (14). During the initial iterations, however, it is evaluated as a weighted sum of the first two heat-transfer-rate estimates to facilitate convergence. The convergence rate depends on the physical models employed.

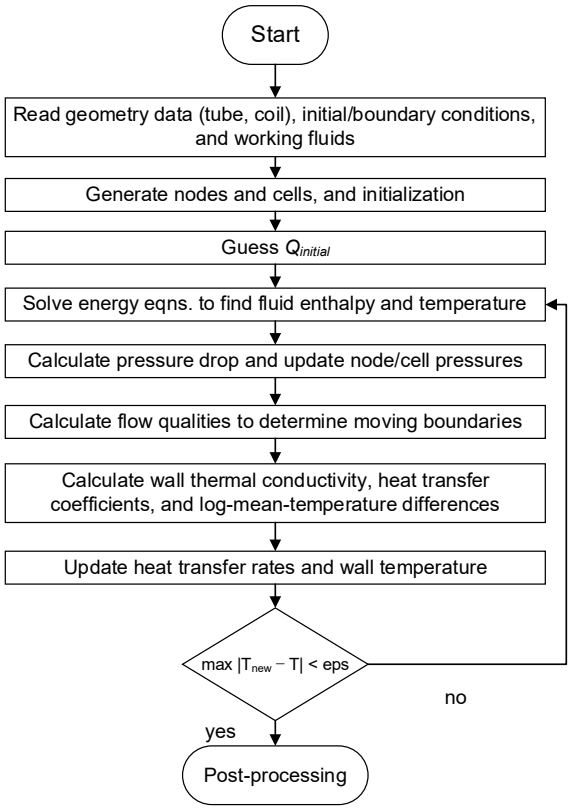


Fig. 2. HCOTSG Calculation procedure

To evaluate the physical models for the HCOTSG, many available models are implemented into and tested using the developed program, as summarized in Table 1. Many of the models are well-known and widely used in the thermal-hydraulic analysis codes. Some of them have strong physical bases (e.g., Mori-Nakayama, Chen, and PNU), and the others are empirically developed from experimental data (e.g., Zukauskas). Only a few good models are available for the shell-side characteristics.

Table 1: Summary of used physical models [3–7]

Variable		Tube-side	Shell-side
Heat transfer	Convective to liquid	Mori-Nakayama*, Schmidt	Zukauskas* Gnielinski
	NVG	Saha-Zuber	
	Fully developed	Thom, Mori-Nakayama*	
	Nucleate boiling	Chen*, PNU	
	Mist	Linear interpolate	
	Dryout	Biasi*, Santini et al. (2014) Xia et al. (2017)	
	Convective to vapor	Bishop*, Gnielinski, Schmidt	
Pressure drop	Friction factor	Colebrook-White, Mori-Nakayama*, Ito, PNU, Schmidt, Santini (2008)	Zukauskas*
	Two-phase multiplier	Jones*, Lockhart-Martinelli, PNU, Zhao	

(* *Default model*)

3. Verification and Valuation Results

The developed HCOTSG program was verified against the MRX steam generator data, which uses water as the working fluid on both the primary and secondary sides [2]. Comparison with the previous studies exhibit a good agreement in the temperature distribution as presented in Fig. 3 and Table 2. Small discrepancies are observed in the boundary of the superheated region and in the temperature distribution within this region. The calculated tube-side pressure drop is ~4.6 bar (~30% < design value). Most previous studies focused primarily on heat transfer perspective rather than pressure drop characteristics.

The physical models were assessed using the developed program, and the results are shown in Figs. 4–7. For tube-side boiling heat transfer, the HTC predicted by the Chen model was high, increasing to 50 kW/m²·K over the first half of the boiling region and decreasing near its end as the working fluid approached the superheated state. An abrupt change was observed near the mist-flow region. This finding is similar to the MARS-KS and SPACE results presented in Ref. [1]. The HTC predicted by the PNU model was much lower and showed the opposite trend. The PNU model correlates experimental data, mostly below 20 kW/m²·K, by adding a term accounting for centrifugal force to the single-

phase HTC calculated using the Dittus–Boelter correlation. Because of the low HTC, the superheated-region boundary shifts toward the tube outlet, and the superheated state may not be reached.

Table 2. Typical MRX calculation results

MRX	Q [MW]	ΔP_p [bar]	ΔP_s [bar]	$T_{p,o}$ [℃]	$T_{s,o}$ [℃]
Design	100	-	6.4	282.5	289.0
Yoon et al. (2000)	-	0.12	4.5	282.5	289.0
Kim-Bang (2024)	-	-	-	283.7	281.5
HCOTSG Inline	99.84	1.52	4.64	282.5	288.0
HCOTSG Staggered	99.92	0.006	4.65	282.5	288.6

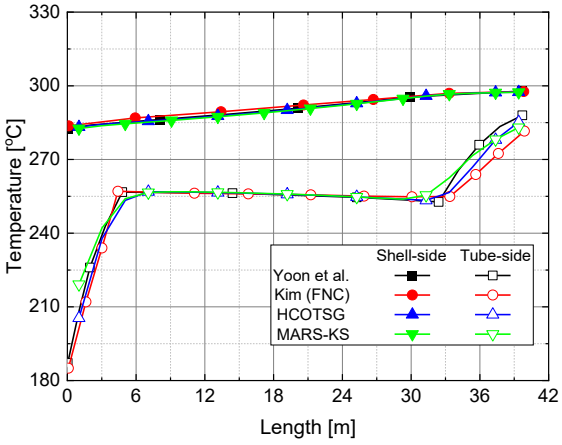


Fig. 3. MRX (inline): Temperature results

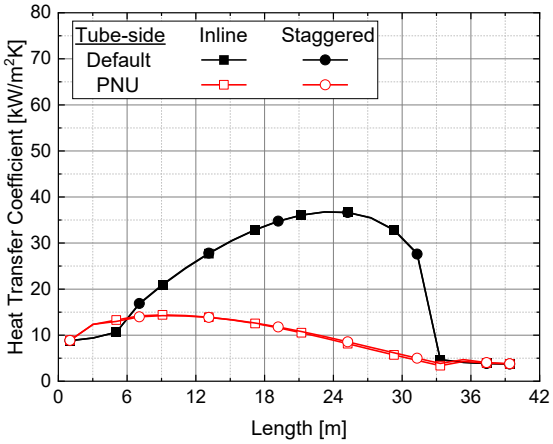


Fig. 4. MRX: Effect of boiling heat transfer models

For shell-side heat transfer, a clear difference in HTC is observed between the inline and staggered tube arrangements. In general, the staggered arrangement produces a higher HTC, depending on the tube pitches. However, the MRX tube arrangement is unknown and was therefore assumed. The Gnielinski correlation appears more suitable because it accounts for the bundle arrangement and the number of tube rows.

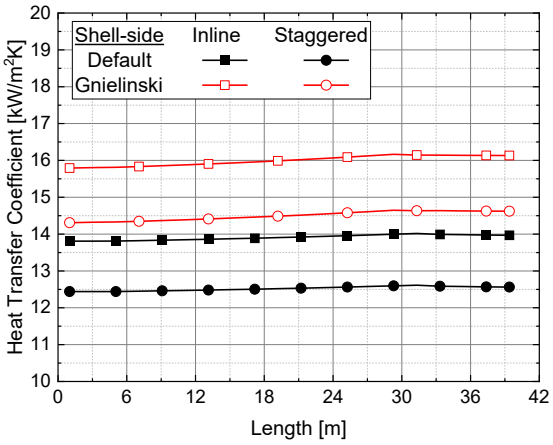


Fig. 5. MRX: Effect of primary heat transfer models

Large differences are observed in the calculated tube-side pressure drop, particularly in the frictional pressure drop (Figs. 6–7). Among the friction-factor correlations, only the Colebrook–White and Schmidt correlations predicted large pressure drops. Regarding the two-phase friction multiplier, the correlations based on the homogeneous flow model (i.e., Jones and Colebrook–White) predicted an increase in pressure drop along the helical tubes. The other correlations predicted a decrease in the mist-flow and superheated regions.

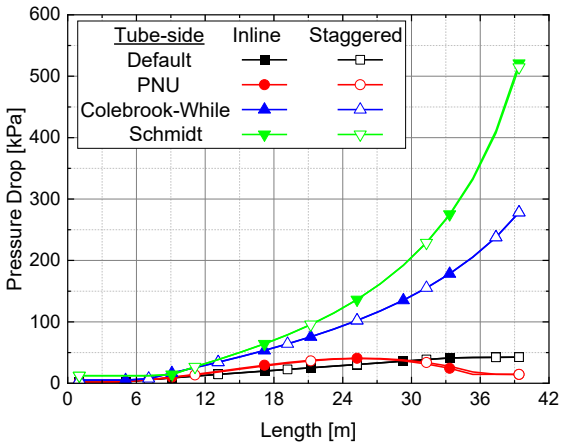


Fig. 6. MRX: Effect of tube-side friction factor models

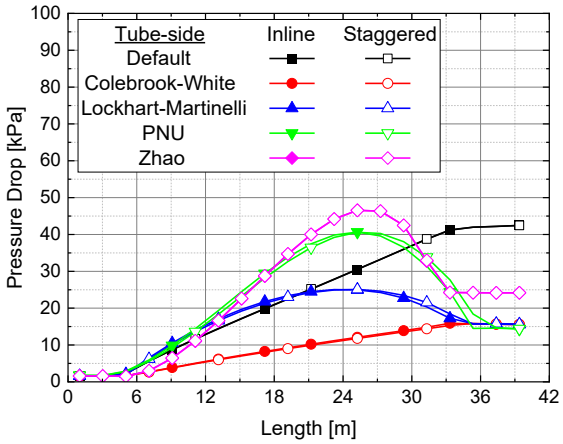


Fig. 7. MRX: Effect of ϕ_{lo}^2 models

In fact, a high tube-side pressure drop, up to several MPa, is often reported. Among the correlations, only the combination of the Schmidt friction factor and Jones two-phase friction multiplier predicts such a high pressure drop. However, the two-phase friction multiplier decreases significantly to below 10 with increasing pressure [7]. Therefore, predicting a high tube-side pressure drop remains difficult.

The assessment indicates large uncertainties in the physical models and a lack of reliable models and experimental data. In addition, the physical parameters used in the models should be clearly defined.

The following results present the validation of the developed program against the VISTA experimental data, which also uses water as the working fluids on both the primary and secondary sides [8]. The Colebrook–White and Schmidt friction-factor correlations were considered to obtain comparable tube-side pressure drops. The calculated heat-transfer rate, shell-side pressure drop, and primary outlet temperature agree well with the experimental data, as shown in Figs. 8–10. The measured tube-side pressure drop fell between the results calculated using the two correlations. The calculated secondary outlet temperature was higher than the measured value, possibly because of the difference in pressure drop.

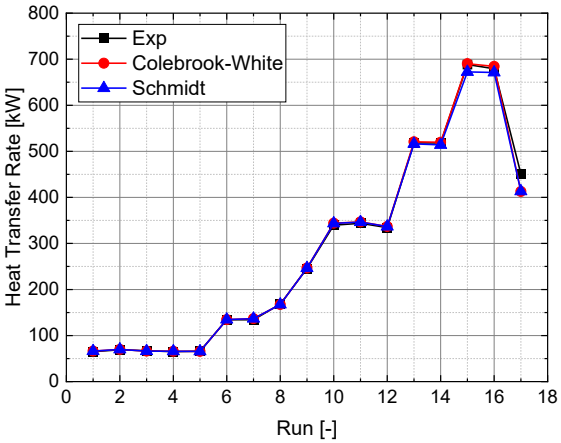


Fig. 8. VISTA: Heat transfer rate results

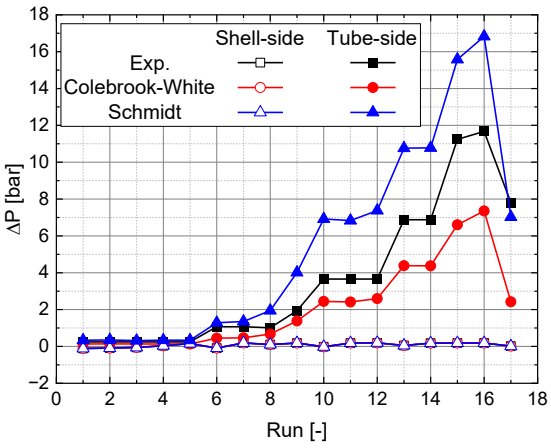


Fig. 9. VISTA: Pressure drop results

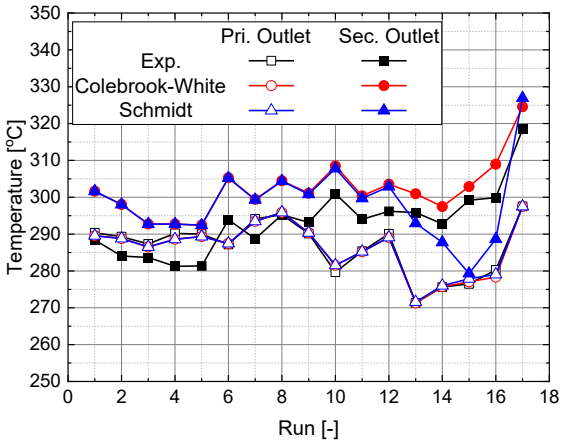


Fig. 10. VISTA: Temperature results

4. Conclusion

This study developed a thermal-hydraulic program for HCOTSG design analysis based on the homogeneous-flow model. The program was evaluated using various combinations of physical models for HCOTSG heat transfer and pressure drop. The verification and validation demonstrated its adequate capability for HCOTSG design analysis while highlighting the lack of reliable physical models and experimental data. Therefore, careful assessment and selection of the physical models are necessary when using the developed program.

ACNOWLEDGEMENTS

This work was supported by the National Research Foundation of Korea (NRF) granted by the Korea government (MSIT) (No. RS-2024-00457356).

REFERENCES

[1] S. Joo, D. H. Kim, S. Oh, J. H. Hwang, and J. I. Lee, Comparison of MARS-KS and SPACE Code for Modeling a Helical Steam Generator, Transactions of the KNS Autumn Meeting, Changwon, Korean, Oct. 24-25, 2024.

[2] J. Yoon, J. P. Kim, H. Y. Kim, D. J. Lee, and M. H. Chang, J. Nuc. Sci. Tech. Vol. 37, pp. 445-454, 2000.

[3] J. G. Collier and J. R. Thome, Convective Boiling and Condensation, Claren Don Press, 1994.

[4] K. Y. Kim and Y. S. Bang, Development and application of the helically coiled once-through steam generator module for dynamic simulation of nuclear hybrid energy system, Nuc. Eng. Tech., vol. 56, pp. 3315-3329, 2024..

[5] Heat Exchanger Design Hanbook, Hemisphere, 1983.

[6] J. J. Jeong, T. G. Lee, S. G. Nam, and B. J. Yun, Incorporating the Effect of Centrifugal Force into the Correlation for Saturated Flow Boiling Heat Transfer in a Helically Coiled Tube, Nuclear Technology, vol. 211, pp. 1875-1882, 2025.

[7] O. Zidi, B. J. Yun, and J. J. Jeong, Development of Frictional Pressure Drop Correlation for Single- and Two-phase Flow in Helically Coiled Tube, Transactions of the KNS Autumn Meeting, Changwon, Korean, Oct. 24-25, 2024.

[8] S. H. Yang, S. H. Kim, Y. J. Chung, H. S. Park, and K. K. Kim, Experimental validation of the helical steam generator model in the TASS/SMR code, Annuals of Nuclear Energy, vol. 35, pp. 49-59.